Pesticide Biochemistry and Physiology 157 (2019) 45–52

Contents lists available at ScienceDirect

Pesticide Biochemistry and Physiology

journal homepage: www.elsevier.com/locate/pest

An insight into the mechanism of antifungal activity of biogenic nanoparticles than their chemical counterparts

Madhuree Kumari[a,d,1], Ved P. Giri[a,c,1], Shipra Pandey[a,d], Manoj Kumar[b], Ratna Katiyar[c], Chandra S. Nautiyal[a], Aradhana Mishra[a,*]

[a] CSIR-National Botanical Research Institute, Rana Pratap Marg, Lucknow 226 001, India
[b] CSIR-Indian Institute of Toxicology Research, Vishvigyan Bhawan 31, Mahatma Gandhi Marg, Lucknow 226 001, India
[c] Department of Botany, Lucknow University, Hasanganj, Lucknow 226 007, India
[d] Academy of Scientific and Innovative Research (AcSIR), Ghaziabad 201002, India

ARTICLE INFO

Keywords:
Biogenic silver nanoparticles
Antifungal
Alternaria brassicicola
Reactive oxygen species
Membrane disintegration

ABSTRACT

Herein, we describe the enhanced antifungal activity of silver nanoparticles biosynthesized by cell free filtrate of *Trichoderma viride* (MTCC 5661) in comparison to chemically synthesized silver nanoparticles (CSNP) of similar shape and size. Biosynthesized silver nanoparticles (BSNP) enhanced the reduction in dry weight by 20 and 48.8% of fungal pathogens *Fusarium oxysporum* and *Alternaria brassicicola* respectively in comparison to their chemical counterparts (CSNP). Nitroblue tetrazolium and Propidium iodide staining demonstrated the higher generation of superoxide radicals lead to higher death in BSNP treated fungus in comparison to CSNP. Scanning electron microscopy of *A. brassicicola* revealed the osmotic imbalance and membrane disintegrity to be major cause for fungal cell death after treatment with BSNP. To gain an insight into the mechanistic aspect of enhanced fungal cell death after treatment of BSNP in comparison to CSNP, stress responses and real time PCR analysis was carried out with *A. brassicicola*. It revealed that generation of ROS, downregulation of antioxidant machinery and oxidative enzymes, disruption of osmotic balance and cellular integrity, and loss of virulence are the mechanisms employed by BSNP which establishes them as superior antifungal agent than their chemical counterparts. With increasing drug resistance and ubiquitous presence of fungal pathogens in plant kingdom, BSNP bears the candidature for new generation of antifungal agent.

1. Introduction

Fungi are a predominant kingdom known for their ubiquitous presence in any habitat. By creating destruction of crop productivity and human health (Segorbe et al., 2017; Kumari et al., 2017a; Fletcher et al., 2006; May et al., 2016) pathogenic fungi have played havoc inextricably with human evolution. With the ability to adapt any stress condition and accordingly production of virulence factor and encrypting gene rearrangements, gives some of them a unique ability to develop resistance against traditional fungicides up roaring for an effective and immediate strategy against fungal pathogens (Segorbe et al., 2017; Hartmann et al., 2017). Our understanding and response activities have not kept pace with the threats to overcome the pathogenic fungal menace. Silver nanoparticles have emerged as new generation of antimicrobial agents (Kumari et al., 2017a; Kumari et al., 2017b). Their ability to kill a wide range of pathogens encompassing fungi (Kim et al., 2009a; Xue et al., 2016) has made them an inevitable substitute for conventional fungicides. Kim et al. (Kim et al., 2009a) described membrane disruption and cell cycle arrest as the major mechanism of silver nanoparticles employed against *Candida albicans*. ROS dependent fungal cell death has been elucidated behind the fungicidal activity of Ag@ZnO core-shell nanocomposites against *Candida krusei* by Das et al. (Das et al., 2016).

Several strategies have been employed to enhance the antimicrobial potential of silver nanoparticles including modification of surface charge and potential, shape, size modification and manipulation of surface capping (Kumari et al., 2017b; Kvítek et al., 2008). Biosynthesis of silver nanoparticles and their antifungal effects are reported far and wide, but the mechanisms employed during fungal inhibition are still a challenge to unearth. Moreover, a detailed mechanistic investigation of antifungal mechanism comparing silver nanoparticles synthesized by biological and chemical methods is yet to be discovered.

* Corresponding author at: Division of Plant Microbe Interactions, CSIR- NBRI, Rana Pratap Marg, Lucknow 226 001, India.
E-mail addresses: mishramyco@yahoo.com, mishra.a@nbri.res.in (A. Mishra).
[1] Authors contributed equally to this work.

https://doi.org/10.1016/j.pestbp.2019.03.005
Received 13 June 2018; Received in revised form 9 February 2019; Accepted 4 March 2019
Available online 05 March 2019
0048-3575/

Biosynthesis of nanoparticles, being economical and eco-friendly (Mishra et al., 2014; Kumari et al., 2016) have given an easy substitute to nanoparticles synthesized from troublesome chemical methods. Biological moieties, if carefully chosen during nanoparticles biosynthesis can enhance the desired effects of concerned particles. Recently, our group elucidated role of antimicrobial metabolites of *Trichoderma viride* in enhancing the antibacterial potential of silver nanoparticles synthesized from them, than their chemical counterpart (Kumari et al., 2017b). It was clearly observed that biologically synthesized particles could inhibit bacterial growth more efficiently (Kumari et al., 2017b).

This study further explores the potential of biosynthesised silver nanoparticles (BSNP), coated with antimicrobial metabolites of *T. viride* (Kumari et al., 2017b) as a potent antifungal agent. Furthermore, the mechanism employed during fungicidal activity of BSNP in comparison to their chemical counterpart (CSNP) has also been elucidated.

2. Materials and methods

2.1. Materials

Biosynthesized silver nanoparticles (BSNP) and chemically synthesized silver nanoparticles (CSNP) used in this study were synthesized and characterized as reported in our earlier study (Kumari et al., 2017b). Particles were filtered through 0.22 µm syringe millipore filters and sonicated for 2 min before use for getting monodispersed population and remove bulk materials. Nitroblue tetrazolium chloride (NBT) was purchased from Sigma Aldrich, India. Potato dextrose agar (PDA) and potato dextrose broth (PDB) were purchased from HiMedia, Mumbai, India. All other chemicals used in this study were of analytical grade. Fungal cultures of *Alternaria brassicicola* and *Fusarium oxysporum* were obtained from NBRI repository and maintained on PDA slants on 4 °C until further use.

2.2. Concentration dependent inhibition by BSNP

Plates of PDA were prepared, supplemented with 5, 10, 20 and 25% of biogenic silver nanoparticles (1, 2, 4 and 5 µg/mL) (Stock-0.02 mg/mL) and growth inhibition of pathogenic fungi *F. oxysporum* and *A. brassicicola* in comparison to non-supplemented plated was observed after 3rd day of inoculation. Similarly, broth assay was also performed and reduction in dry weight and spore count was measured.

2.3. Comparison of antifungal activity of BSNP and CSNP

For antifungal activity, PDA plates were prepared supplemented with 25% of BSNP and CSNP from the stock of 0.02 mg/mL. A bid of pathogenic fungi *F. oxysporum and A. brassicicola* was placed in the centre and inhibition was measured comparing them with control plate after day 3 of inoculation.

For broth assay, PDB was supplemented with BSNP and CSNP as described earlier. A bid of pathogenic fungus was inoculated in above prepared broth. Reduction in dry weight and spore count was calculated after day 3 of inoculation. Plates supplemented with similar concentration of *T. viride* extract, silver nitrate and without any supplementation served as control.

2.4. Nitroblue Tetrazolium (NBT) reduction assay

To detect superoxide radical by reduction of NBT into the monoformazan (NBT^+), NBT assay was carried out with modified protocol of Rispail et al. (Rispail et al., 2014). Briefly, 1 mL aliquot of threedays old cell suspension culture of *A. brassiccicola* treated with 20% BSNP and CSNP separately for 48 h were transferred to a sterile 1.5 mL eppendorf tube and added with 0.5 mM NBT. All samples were then incubated in an orbital shaker at 180 rpm, in the dark, at 28 °C for 4 h before observation under a bright field microscope (Leica Microsystems, GmbH, Germany) under 100×.

2.5. SYTO9/PI staining and fungal cell membrane integrity

Viability of fungal mycelia were assessed using the Molecular Probes' LIVE/DEAD Fungal Light Viability kit with some modification of Jin et al. (Jin et al., 2005). The LIVE/DEAD kit includes differential stains SYTO9, a green nucleic acid stain, intact with live and dead fungal mycelia. Second dye, red-fluorescent propidium iodide penetrates only dead mycelia.

Fungal mycelia were treated with CSNP and BSNP for 24 h and then washed with phosphate buffer saline (pH 7.4). After washing, mycelia was centrifuged at 5000 rpm for 5 min. 300 µL of each aliquot was treated with 1:1 ratio of SYTO9 (3.34 mM) & PI (20 mM) stains, respectively. Untreated fungal mycelia served as control. Samples were kept in dark for 30 min at 37^0C. Treatments were observed under the fluorescent microscope (EVOS FLc, cell imaging system, Thermo Fischer Scientific).

Integrity of fungal cell membrane was measured by UV–vis spectroscopy following the protocol of Dasgupta and Ramalingam (Dasgupta and Ramalingam, 2016) with some modifications. If fungal cell membrane is compromised, amount of nucleic acid released from cytoplasm can be detected in cell free filtrate. Briefly, after 48 h incubation with 20% BSNP and CSNP, the fungal cell free filtrate was collected and filtered with 0.45 µ syringe filter. The concentration of nucleic acid (DNA) present in cell free filtrate was recorded on NanoDrop (Thermo Scientific, Nanodrop 1000, Spectrophotometer).

2.6. Stress responses of A. brassiccicola upon treatment with BSNP and CSNP

Non enzymatic stress parameters in terms of lipid peroxidation and stress enzyme activities of *A. brassiccicola* upon treatment with 20% BSNP and CSNP for 48 h were estimated following the protocols of Kumari et al. (Kumari et al., 2017a). Briefly, lipid peroxidation (LPX) was determined by estimating content of thiobarbituric acid reactive substances (TBARS). The concentration of TBARS was calculated by using the extinction coefficient of 155 $mM^{-1}\,cm^{-1}$. One unit of Superoxide dismutase (SOD) activity was expressed as the amount of protein required to inhibit 50% of initial reduction of NBT under light. Catalase activity was recorded as decrease in the absorbance of H_2O_2 at 240 nm (extinction coefficient 0.04 $m^2\,\mu mol^{-1}$) and enzyme activity was expressed as u/min/mg of protein. Ascorbate peroxidase (APX) was measured as change in absorbance at 290 nm and expressed as u/min/mg of protein. Guaiacol peroxidase (GoPX) activity was measured as increase in absorbance due to oxidation of guaiacol (extinction coefficient 26.6 $mM^{-1}\,cm^{-1}$) at 470 nm and expressed as u/min/mg of protein.

2.7. Scanning Electron Microscopy (SEM)

SEM observations were carried out following the protocol of Pochon et al. (Pochon et al., 2012) with some modifications. In 100 mL of PDB, bid of *A. brassicicola* was inoculated and allowed to grow for three days. After 3rd day of inoculation, the flasks were supplemented with 20% of BSNP and CSNP from stock solution in different flasks for 48 h, while in control flask; 20 mL of MQ water was added. Fungal mycelia grown were filtered and were fixed under vacuum in 4% (v/v) glutaraldehyde in 0.1 M phosphate buffer (pH 7.2) for 24 h at 4 °C. Further specimen was fixed in 2% (w/v) osmium tetraoxide in 0.1 M phosphate buffer and dehydrated in a graded ethanol series (50, 70, 95 and 100% for 10 min each). The last dehydration step was repeated three times and dried by the critical- point method. Samples were then sputter coated with a thin carbon layer and examined using a Quanta FEG 450 (FEI, Netherlands) scanning electron microscopy.

Table 1
List of primers used in this study.

Name of the primer	Primer sequence	Gene Bank ID	Source
SOD (Superoxide dismutase)	abSOD-expFor 5'GCAAAATTGCTCCTCCTTTG abSOD-expRev 5'TGCCAGACTGGTGACTTGAG	AB07556.1	JGI
TRX2 (Thioredoxin)	abTRX-expFor 5'AGAGCCACCAGAACACTGCT abTRX expRev 5'CGACGGGATTTCAACTCACT	AB00422.1	JGI
GSH2 (Reduced Glutathione)	abGSH-expFor 5'ATGGTGCATCAAGACCCTTC abGSH -expRev 5'AGAGCCTCGTGCTTGATGAT	AB09076.1	JGI
TmPL (Damage Induced Oxidative stress)	abATM1-expFor 5'TCTGAAGTAACACCAGGCAAGGGT abATM1-expRev 5'TCCATATATGTGTCGGCGCGGTAT	EU223383	NCBI
abNPS2 (Cell wall intrigrity)	abNPS2-expFor 5'ACTTTCAATCGCTCGCCATC abNPS-expRev 5'AGCTTGCTTCAACTTGCGAA	EU090010	NCBI
abNIK1 (Osmoregulation)	abNIK1-expFor 5'AGATGTCGGAACTGAAGGCA abNIK1-expRev 5'CCTGGGTGGTAAGGTTTTGC	AY700092	NCBI
abAMK1 (MAP Kinase, Cell division)	abAMK1-expFor 5'CATGTTCCCCAAGACCAACG abAMK1-expRev 5'TCTGGATCATGGTACGGCTC	AY515257	NCBI
abSlt2 (Cell wall intigrity)	abSlt2-expFor 5'CTACCGTACATGCAGAAGATC abSlt2-expRev 5'AGGCATCGTGCCAGATTTGTAGGT	AY705975	NCBI
GAPDH (Glyceraldehyde 3 phosphodehydrogenase)	GAPDH-For 5'TGGAAAGAACCTCGATGTCGGACT GAPDH-Rev 5'ACGTTGTTGAGTCCACTGGTGTCT	MG250616	NCBI

2.8. Real time PCR (RT-PCR)

For the expression studies, two-step RT-PCR was performed with 5 µg of total RNA, which was isolated from treated and non-treated fungal biomass using Trizol (*Invitrogen*) with manufacturer's instructions. The first strand of cDNA was synthesized with a Reverse Transcription System (Promega), and this was subsequently used as a template for Real Time PCR with gene-specific primers (Table 1) (Kim et al., 2009b; Xu, 2000) on Step One Real Time PCR system (Applied Biosystem). Five flasks of each treatments were randomly selected and pooled for isolation of RNA in triplicate. The cycling conditions were as follows: denaturation was done at 94 °C for 5 min for one cycle; however, for 40 cycles denaturation was done for 30 s. Annealing was done at 60 °C for 30 s, and extension at 72 °C for 60 s. Glyceraldehyde 3 phosphodehydrogenase gene was used as a reference gene. *Statistical analysis.*

All the experiments were performed in triplicate and quantitative variables are represented in terms of means ± S.D. in histograms. The statistical significance for the different treatments was determined by one-way ANOVA post hoc Bonferroni multiple comparison test (SPSS 11.5.0, USA) with probability of *P*-value of ≤ 0.05.

3. Results and discussion

3.1. Concentration dependent antifungal activity by BSNP

For assessing the antifungal properties of BSNP, fungal isolates of *A. brassicicola* and *F. oxysporum* were selected because of their ubiquitous presence and ability to cause disease in both animal and plant system. *Alternaria* sp. are known plant pathogen and common allergen to human (Gauthier and Keller, 2013; Babiceanu et al., 2013), while *F. oxysporum* is also a crossover fungi capable of crossing kingdoms to infect plants and humans (Gauthier and Keller, 2013; López-Berges et al., 2013). BSNP demonstrated dose dependent antifungal activity against *F.oxysporum* and *A.brassicicola* (Fig. S1). Five percent BSNP of silver nanoparticles was effective enough to suppress their growth while 25% of particles completely inhibited the pathogen on plate assay (Fig. S1).

Similar results were also observed in broth assay (Fig. S2). With 25% of BSNP, reduction of 90 and 57% in dry weight of *A. brassicicola* and *F. oxysporum* respectively were obtained (Fig. S2a). 20% of BSNP were sufficient to inhibit spore formation in *A. brassicicola* while 25% of BSNP were able to reduce the conidia of *F. oxysporum* by 98% (Fig. S2b). Toxic effects of silver nanoparticles on reproductive system are exploited in some systems which can be utilized to inhibit the survival of plant pathogenic fungi.

3.2. Antifungal activity of BSNP in comparison to CSNP

BSNP showed better inhibition of fungal pathogens as compared to CSNP in plate assay (Fig. 1). The antifungal activity was highest in BSNP in comparison to CSNP, aqueous silver nitrate and cell free extract of *T. viride.*

In broth assay, the results obtained were in accordance with plate assay (Fig. 1b). Reduction in dry weight was 20% and 48.8% higher with BSNP as compared to CSNP in *F. oxysporum* and *A. brassicicola* respectively (Fig. 1b). The activity of BSNP was higher by 23.55 and 39.8% in *F. oxysporum* and *A. brassicicola* respectively in comparison to silver nitrate. The susceptibility of *A. brassicicola* was more towards the antimicrobial metabolites produced by *T. viride* as compared to *F. oxysporum* which might be a reason of enhanced antimicrobial potential of BSNP against *A. brassicicola* in comparison to *F. oxysporum.*

There was enhanced reduction in spore count of *F. oxysporum* by 18.8% after 3 days of inoculation with BSNP as compared to CSNP, while with *A. brassicicola*, the fungus was unable to form the spores in presence of BSNP even after 3 days of incubation while spore formation took place in case of CSNP (Fig. 1c). The antimicrobial activity of silver nanoparticles alone in CSNP was not able to suppress growth of spores, but BSNP treatment, having supplementation of *T. viride* metabolites completely inhibited the germination of spores. The proteins and metabolites secreted by *Trichoderma* sp. itself plays an antifungal role and have widely been used in agriculture to control plant pathogens (Harman et al., 2004; Yan et al., 2006). BSNP having synergistic effects of both, amylolytic, proteolytic activities and metal chelation of cell free extract of *T. viride* (Kumari et al., 2017b) and DNA unwinding, membrane disruption and binding with important biological molecules by SNP (Perkas et al., 2013) would become a challenge for pathogen to survive and gain resistance against BSNP.

3.3. Nitroblue Tetrazolium (NBT) reduction assay

To gain a mechanistic insight, *A. brassicicola* was selected for further studies because of its higher susceptibility towards BSNP.

Nitro substituted aromatics such as Nitroblue Tetrazolium salts are used to detect superoxide radicals. NBT is reduced by $O_2^{-\bullet}$ to the monoformazan (NBT^+), visible as accumulation of dark blue spots of formazan (Rispail et al., 2014). In this study, prominent accumulation of formazan was visible in BSNP and CSNP treated fungal mycelia (Fig. 2b,c). Structural aberration in fungal mycelia with production of superoxide radicals was clearly evident in BSNP treated *A. brassicicola.*

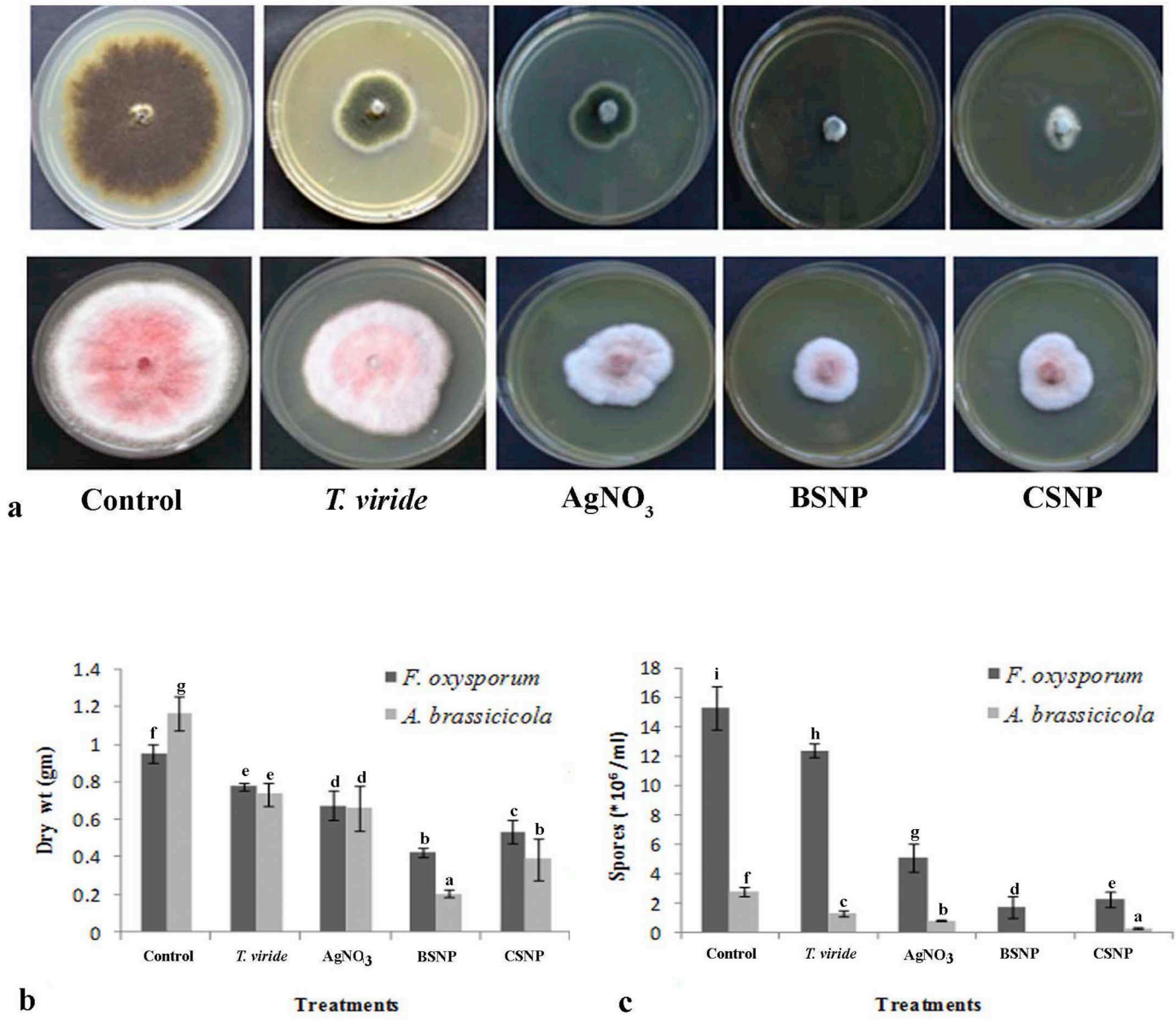

Fig. 1. Antifungal properties of BSNP as compared to CSNP against *F. oxysporum* and *A. brassicicola* (a) plate assay (b) dry weight of *F. oxysporum* and *A. brassicicola* after treatment with *T. viride* extract, $AgNO_3$, BSNP and chemically synthesized silver nanoparticles (CSNP) (c) spore count of *F. oxysporum* and *A. brassicicola* after treatment with *T. viride* extract, $AgNO_3$, BSNP and CSNP. Values are the means ± SD of three replicates. Means sharing different alphabets "a", "b" differ significantly from each other at $p \leq .05$.

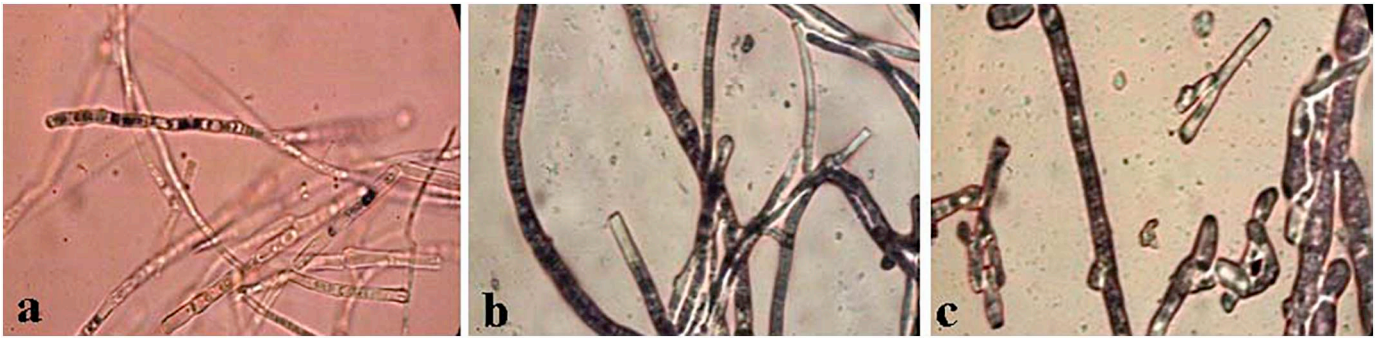

Fig. 2. Assessment of O^{2-} generation on *A. brassicicola* following treatment with (a) Healthy mycelia without any treatment (b) CSNP (c) BSNP.

Table 2
Release of DNA in cell free filtrate after treatment with BSNP and CSNP.

Treatment	Concentration of DNA (μg/μL)
Control	199.9 ± 9.9[a]
BSNP	533.8 ± 35.4[c]
CSNP	382.2 ± 42[b]

Values are the means ± SD of three replicates. Means sharing different alphabets "a", "b" differ significantly from each other at $p \leq .05$.

Generation of $O_2^{-\bullet}$ is largely responsible for inducing oxidative stress (Rispail et al., 2014) which can further induce membrane, DNA and protein damage ultimately leading to cell death.

3.4. Integrity of fungal cell membrane

Nanoparticles are known to disturb fungal cell membrane integrity as one of their fungicidal mechanism (Kumari et al., 2017b). Damaged cell membrane results in leaching of nucleic acid and other ions into cell free filtrate (Dasgupta and Ramalingam, 2016). Concentration of DNA in cell free filtrate was most abundant in BSNP treated fungus followed by CSNP treatment (Table 2) as observed during nano drop readings in comparison to un-treated control. Increased ROS generation during BSNP treatment can account for enhanced membrane disintegration and subsequently increased leakage of DNA in cell free filtrate.

3.5. SYTO9/Propidium iodide (PI) staining

PI is a membrane impermeable nucleic acid dye which gets internalized and fluoresce red only when the membrane is compromised (Kumari et al., 2017b). In this study, the PI red fluorescence was maximum in BSNP treated cells, where as in CSNP treated fungal cells, PI fluorescence was minimal after 24 h of treatment (Fig. 3). Healthy un-treated control cells depicted no PI fluorescence. The results firmly corroborated the results obtained earlier with ROS generation and membrane disintegrity.

3.6. Scanning electron microscopy

Scanning electron microscopy also revealed similar observation with NBT reduction assay to elucidate the mechanism of BSNP as superior antimicrobial agent. The intact architecture of *A. brassicicola* was completely disintegrated after BSNP treatment (Fig. 4b,c).

In comparison with CSNP treatment, showing prominent injury to the mycelia, BSNP treated mycelia demonstrated completely damaged or dead cells (4c,d). Since BSNP possess properties of both, silver nanoparticles and cell free extract of *T. viride*, it employs multiple modes of actions including protein degradation, and complete disruption of cell by cellular lyses and disruption of osmotic balance, cell wall leakage as observed in SEM, making it impossible for pathogen to recover after injury resulting in a complete inhibition. The surface modification of nanoparticles in biosynthesis has often been neglected though some attention has been provided on surface manipulation by chemical approach (Diama et al., 2014). This study can provide an insight into the fact that biological means used for biosynthesis of nanoparticles can improve the properties concerned with biosynthesized particles, highlighting the importance of accurate selection of biological agents to get enhanced activity.

3.7. Stress responses of A. brassicicola during interaction with BSNP and CSNP

Lipid peroxidation is direct marker of membrane damage by peroxidation of lipid caused by ROS species (Kumari et al., 2017a). A 108.15% increase in lipid peroxidation was observed with BSNP treated fungal cells in comparison to un-treated control, while the increase was 21.85% in comparison to CSNP treated fungal cells (Fig. 5a). Further, stress enzyme activities of fungal cells decreased drastically upon treatment of BSNP and CSNP in comparison to un-treated control. Activities of SOD, catalase, APX and GoPX decreased to 15.27, 26.59, 70.73 and 42.77% respectively in BSNP treated fungal cells in comparison to CSNP treatment (Fig. 5b,c,d,e). Stress enzymes play a vital role in maintaining redox homeostasis in cells after generation of ROS. The levels of antioxidant enzymes may vary during oxidative stress, either resulting in increase in their activity to combat oxidative stress or decrease in their activity upon failure to reduce stress and denaturation of concerned enzyme and protein (Hua et al., 2017). Hua et al. (Hua et al., 2017) found a decrease in SOD enzyme activity upon infection of *C. albicans* causing increased oxidative stress in inflamed corneal tissue. Earlier, Yu et al. (Yu et al., 2009) also reported decreased antioxidative activity resulted in increased mitochondrial DNA damage in cellular models of Machado-Joseph Disease.

3.8. Quantitative PCR analysis

To elucidate the molecular basis of higher antifungal activity of BSNP in comparison to CSNP, real time PCR analysis was carried out. The expression analysis of eight genes involved in antioxidant machinery, cell wall integrity, osmotic balance and antioxidative enzymes were studied in BSNP and CSNP treated mycelia of *A. brassicicola*.

All the eight genes studied depicted a differential expression profiles

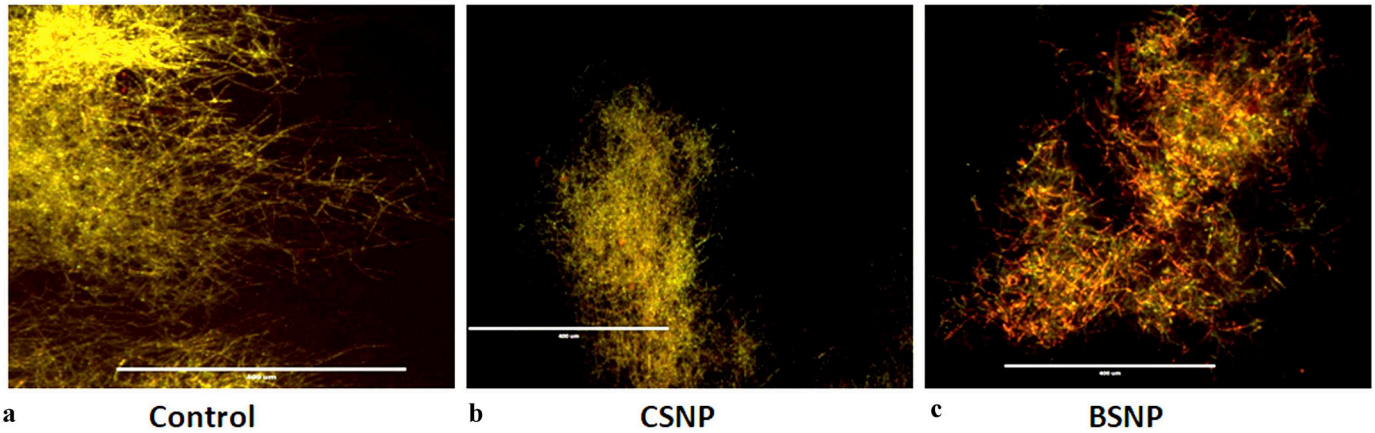

Fig. 3. SYTO9/PI staining of *A. brassicicola* fungal mycelia following treatment with (a) Healthy mycelia without any treatment (b) CSNP (c) BSNP.

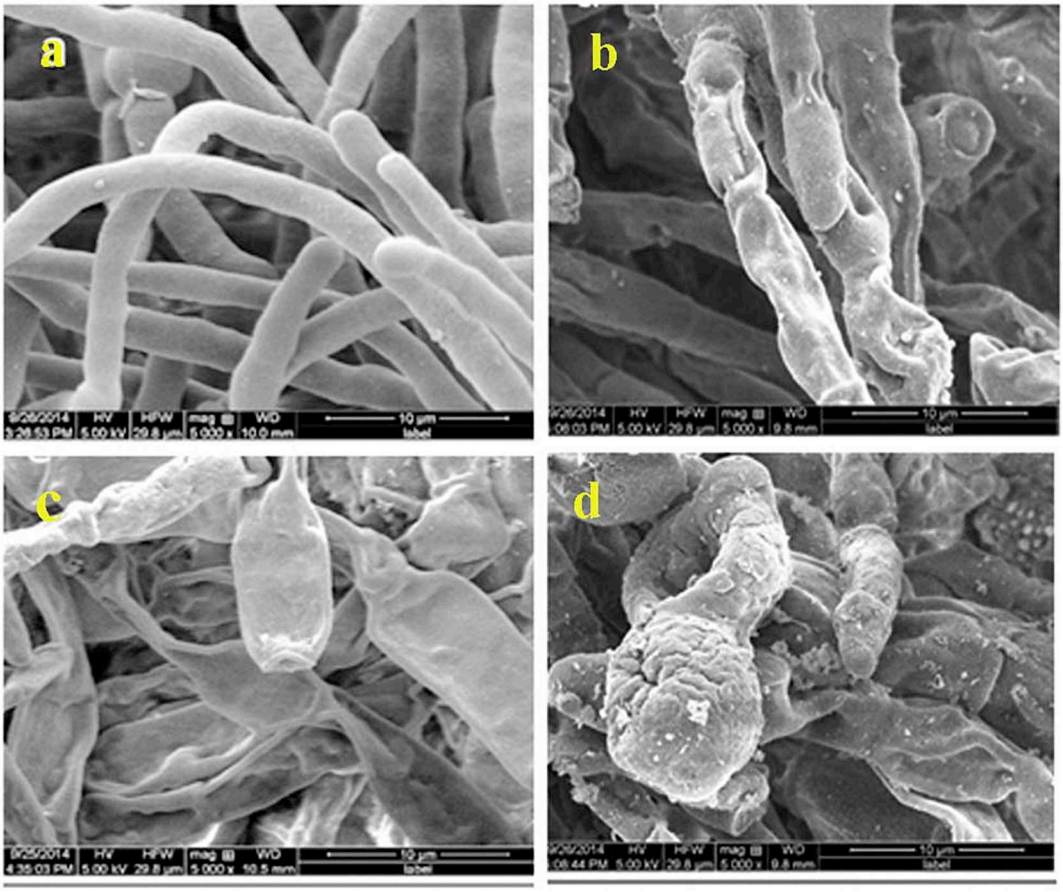

Fig. 4. SEM micrograph of *A. brassicicola* (a) Healthy mycelia network without any treatment (b) CSNP treated partially damaged mycelia (c) (d) BSNP treated completely damaged mycelia and spores.

in BSNP and CSNP treated fungus (Fig. 6). Glutathione synthetase (*GSH2*) upregulated by 0.19 ± 0.05 $\log_{10}$ fold in CSNP treatment, while BSNP treated fungi showed an upregulation of 0.24 ± 0.04 $\log_{10}$ fold depicting the oxidative stress faced by the fungi due to generation of higher ROS. Further, gene involved in amelioration of oxidative stress, superoxide dismutase (SOD) showed down regulation by one fold when treated with BSNP, while upregulated when treated with CSNP. The results clearly demonstrated the failure of oxidative enzyme to cope up the higher oxidative stress caused by BSNP on pathogenic fungi.

Genes involved in cell wall integrity, osmotic balance, conidial viability, virulence and cell division viz. *NPS2, NIK and AMK* (Kim et al., 2009b; Kim et al., 2007) showed down regulation with treatment of BSNP while up regulation with CSNP treated fungus. BSNP treated fungus completely lost the osmotic balance, cell wall integrity and germination ability while CSNP treated fungus was still coping up with the stress and osmotic imbalance by increasing the expression of genes involved (Fig. 6). BSNP treated fungus also showed significant down-regulation of gene involved in maintaining endogenous antioxidant system *TRX*, while 0.02 ± 0.1 $\log_{10}$ fold down regulate with CSNP treated fungus was observed. The obtained results clearly indicated that CSNP is not much efficient to resist spore germination of *A. brassicicola*, where BSNP proved itself as a potent fungicide. This indicates the adaptation strategies employed by CSNP treated *A. brassicicola* which were able to cope up with oxidative damage while BSNP treated fungus failed to do so, ultimately leading to death of the pathogen. Espinosa-Diez et al. (Espinosa-Diez et al., 2015) have also focussed on role of thioredoxin (*TRX*) in cellular adjustment to oxidative stress, failure of which results in cellular disintegrity.

ATM is responsible for synthesis of transmembrane protein required for intracellular redox homeostasis (Kim et al., 2009b). Down regulation with both CSNP and BSNP treated fungus demonstrates the imbalance in redox homeostasis inside the cell.

Fungal cells trigger adaptive strategies to combat situations that compromise cell wall integrity (García et al., 2017; Malkapur et al., 2017). *SLT2* triggers a cascade of genes in response to stress to maintain the integrity of cell wall. Though CSNP treated cells increased the expression of *SLT2* gene to 15.9 folds to rebuild the cell wall machinery, BSNP treated fungal cells could increase it to 5.1 fold, depicting severe damage leading to loss of osmotic imbalance and cellular integrity.

3.9. Mechanism of higher antifungal activity of BSNP in comparison to CSNP

Based upon the results and observations, higher antifungal activity of BSNP in comparison to CSNP can be attributed to following reasons (Graphical abstract): 1. **Reactive oxygen species (ROS) generation:** BSNP treatment was able to generate higher ROS, especially superoxide radicals as observed by NBT staining. 2. **Down regulation of stress enzymes:** BSNP treatment down regulated the expression of oxidative enzymes resulting in failure to cope up with oxidative stress caused by BSNP 3. **Disruption of endogenic antioxidant machinery:** BSNP treatment completely disrupted the inbuilt redox homeostasis of pathogen, while CSNP treatment failed to do so. 4. **Cell wall disruption and osmotic imbalance:** Altered redox homeostasis and oxidative stress resulted in complete loss of membrane integrity and imbalance in osmotic pressure after treatment with BSNP. Membrane disintegrity, PI staining, Real time PCR and SEM results demonstrated the cells leading to death by loss of membrane structure and osmotic balance in BSNP treated fungus while CSNP treatment resulted in membrane injury not death which can be combated by pathogen.

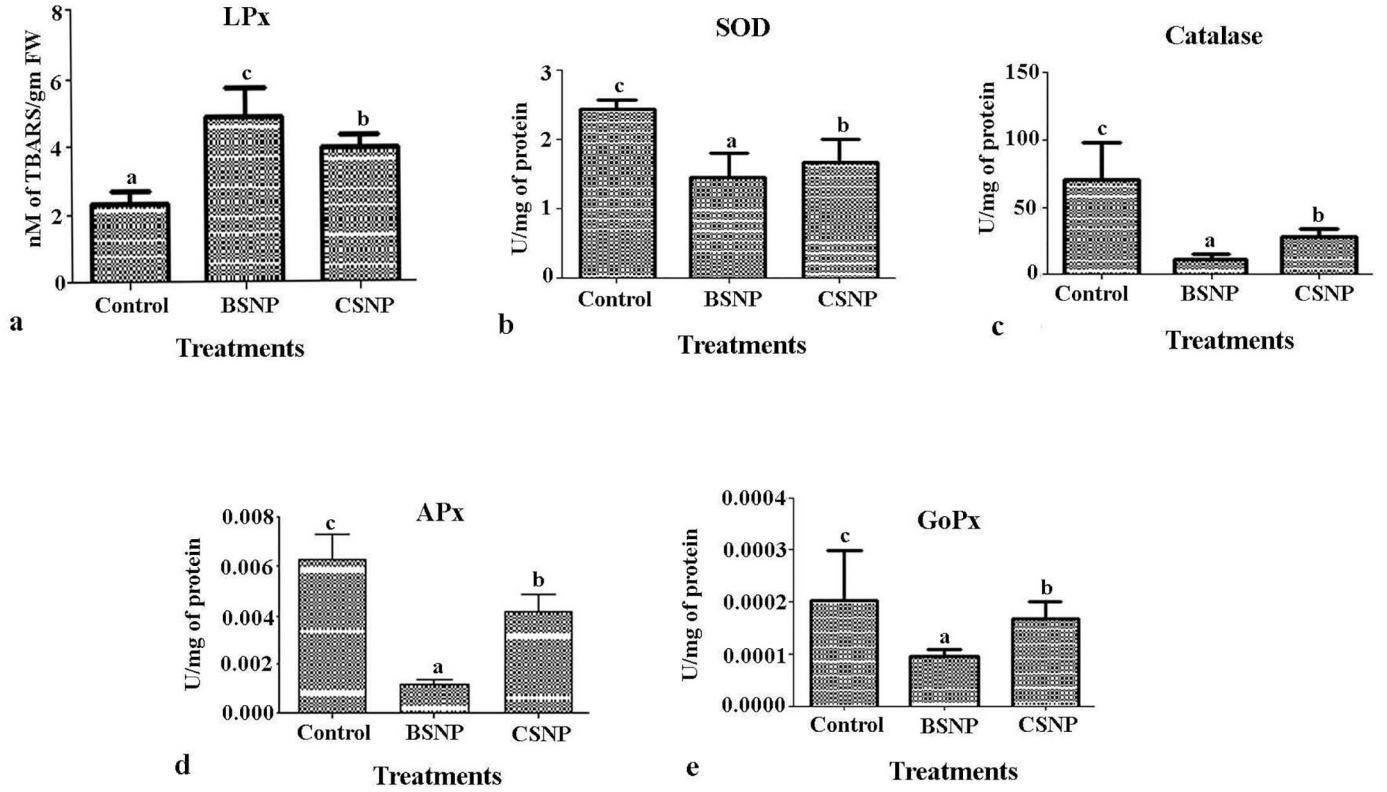

Fig. 5. Stress responses of *A. brassicicola* after treatment with BSNP and CSNP in terms of (a) lipid peroxidation (b) superoxide dismutase activity (c) catalase activity (d) ascorbate peroxidase activity (e) guaiacol peroxidase activity. Values are the means ± SD of three replicates. Means sharing different alphabets "a", "b" differ significantly from each other at $p \leq .05$.

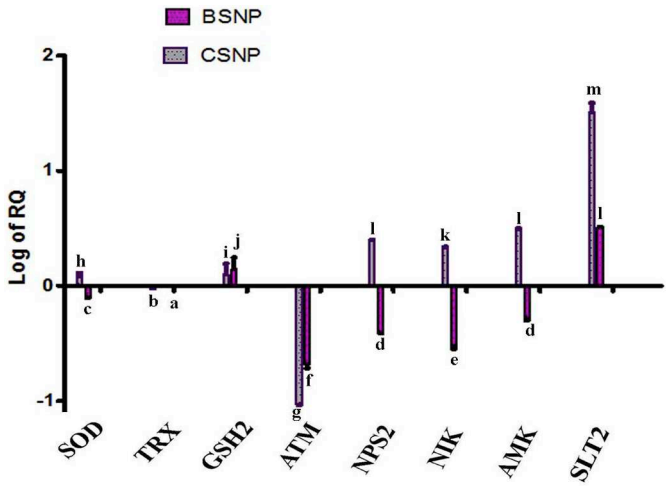

Fig. 6. Differential expression of genes quantified by real time PCR in *A. brassicicola* after treatment with BSNP and CSNP. Values are the means ± SD of three replicates. Means sharing different alphabets "a", "b" differ significantly from each other at p ≤ .05.

BSNP, with properties of silver nanoparticles and coating of antimicrobial metabolites of *T. viride* clearly demonstrated superior antifungal activity than its chemical counterpart. This study can also give an insight into the careful selection of microbial agents while biosynthesis of nanoparticles.

4. Conclusions

This study demonstrated the enhanced antifungal activity of BSNP in comparison to CSNP. The amalgamation of antifungal properties of silver nanoparticles and cell free filtrate of *T. viride* in BSNP served as superior antifungal agent against fungal pathogens *F. oxysporum* and *A. brassicicola*. A concentration dependent inhibition of fungal pathogens was observed after BSNP treatment. Nitroblue tetrazolium assay confirmed the production of superoxide radicals and ROS generation, while scanning electron microscopy revealed disintegration of cellular structure of *A. brassicicola* after treatment of BSNP. Collapse of redox homeostasis, antioxidant machinery, cellular virulence and damage of cell wall and membrane by disrupting osmotic balance as major mechanisms was unveiled by stress enzyme activities and real times PCR studies manifesting the BSNP to act as superior antifungal agent in comparison to CSNP. This study also suggested that if biological agents are chosen carefully, biosynthesis of nanoparticles can enhance the desired effects.

Conflict of interest

The authors declare that they have no conflict of interest.

Acknowledgements

Authors thank Director of CSIR- National Botanical Research Institute, India for his support. Authors are also thankful to CSIR- Indian Institute of Toxicology Research for providing SEM facility. This study was partially funded by network project of Council of Scientific and Industrial Research (CSIR) "BSC-0112 NanoSHE" for RT-PCR. MK[b] thanks to CSIR for awarding her Junior and Senior Research Fellowship (JRF and SRF).

Appendix A. Supplementary data

Supplementary data to this article can be found online at https://doi.org/10.1016/j.pestbp.2019.03.005.

References

Babiceanu, M.C., Howard, B.A., Rumore, A.C., Kita, H., Lawrence, C.B., 2013. Analysis of global gene expression changes in human bronchial epithelial cells exposed to spores of the allergenic fungus, *Alternaria alternate*. Front. Microbiol. 4, 196.

Das, M.I., Khan, R., Jayabalan, S.K., Behera, S., Yun, S.I., Tripathy, S.K., Mishra, A., 2016. Understanding the antifungal mechanism of Ag@ZnO core-shell nanocomposites against *Candida krusei*. Sci. Rep. 6, 36403.

Dasgupta, N., Ramalingam, C., 2016. Titanium dioxide nanoparticles induce bacterial membrane rupture by reactive oxygen species generation. Environ. Chem. Lett. 14, 477–485.

Diama, H.K., Selvakannan, P.R., Kandjani, A.E., Shukla, R., Bhargava, S.K., Bansal, V., 2014. Synergistic influence of polyoxometalate surface corona towards enhancing the antibacterial performance of tyrosine-capped Ag nanoparticles. Nanoscale 6, 758–765.

Espinosa-Diez, C., Miguel, V., Mennerich, D., Kietzmann, T., Sánchez-Pérez, P., Cadenas, S., Lamas, S., 2015. Antioxidant responses and cellular adjustments to oxidative stress. Redox Biol. 6, 183–197.

Fletcher, J., Bender, C., Budowle, B., Cobb, W.T., Gold, S.E., Ishimaru, C.A., Luster, D., Melcher, U., Murch, R., Scherm, H., Seem, R.C., Sherwood, J.L., Sobral, B.W., Tolin, S.A., 2006. Plant pathogen forensics: capabilities, needs, and recommendations. Microbiol. Mol. Biol. Rev. 70, 450–471.

García, R., Bravo, E., Diez-Muñiz, S., Nombela, C., Rodríguez-Peña, J.M., Arroyo, J., 2017. A novel connection between the cell wall integrity and the PKA pathways regulates cell wall stress response in yeast. Sci. Rep. 7, 5703.

Gauthier, G.M., Keller, N.P., 2013. The biology and pathogenesis of fungi capable of crossing kingdoms to infect plants and humans. Fun. Gen. Biol. 61, 146–157.

Harman, G.E., Howell, C.R., Viterbo, A., Chet, I., Lorito, M., 2004. *Trichoderma* species—opportunistic, a virulent plant symbionts. Nat. Rev. Microbiol. 2, 42–58.

Hartmann, F.E., Sánchez-Vallet, A., McDonald, B.A., Croll, D., 2017. A fungal wheat pathogen evolved host specialization by extensive chromosomal rearrangements. ISME J. 11, 1189–1204.

Hua, X., Chi, W., Su, L., Li, J., Zhang, Z., Yuan, X., 2017. ROS-induced oxidative injury involved in pathogenesis of fungal keratitis via p38 MAPK activation. Sci. Rep. 7, 10421.

Jin, Y., Zhang, T., Samaranayake, Y.H., Fang, H.H.P., Yip, H.K., Samaranayake, L.P., 2005. The use of new probes and stains for improved assessment of cell viability and extracellular polymeric substances in *Candida albicans* biofilms. Mycopathology 159, 353–360.

Kim, K.H., Cho, Y., La Rota, M., Cramer Jr., R.A., Lawrence, C.B., 2007. Identification of novel virulence factors associated with signal transduction pathways in *Alternaria brassicicola*. Mol. Plant Pathol. 8, 23–39.

Kim, K., Sung, W.S., Suh, B.K., Moon, S., Choi, J., Kim, J.G., Lee, D.G., 2009a. Antifungal activity and mode of action of silver nano-particles on *Candida albican*. Biometals 22, 235–242.

Kim, K., Willger, S.D., Park, S., Puttikamonkul, S., Grahl, N., Cho, Y., Mukhopadhyay, B., Cramer Jr., R.A., Lawrence, C.B., 2009b. TmpL, a transmembrane protein required for intracellular redox homeostasis and virulence in a plant and an animal fungal pathogen. PLoS Pathog. 5, e1000653.

Kumari, M., Mishra, A., Pandey, S., Singh, S.P., Chaudhry, V., Mudiam, M.K.R., Shukla, S., Kakkar, P., Nautiyal, C.S., 2016. Physico-chemical condition optimization during biosynthesis lead to development of improved and catalytically efficient gold nanoparticles. Sci. Rep. 6, 27575.

Kumari, M., Pandey, S., Bhattacharya, A., Mishra, A., Nautiyal, C.S., 2017a. Protective role of biosynthesized silver nanoparticles against early blight disease in *Solanum lycopersicum*. Plant Physiol. Biochem. 121, 216–225.

Kumari, M., Shukla, S., Pandey, S., Giri, V.P., Bhatia, A., Tripathi, T., Kakkar, P., Nautiyal, C.S., Mishra, A., 2017b. Enhanced cellular internalization: a bacterial mechanism more relative to biogenic nanoparticles than chemical counterparts. ACS-Appl. Mater. Interfaces. 9, 4519–4533.

Kvítek, L., Panáček, A., Soukupová, J., Kolář, M., Večeřová, R., Prucek, R., Holecová, M., Zbořil, R., 2008. Effect of surfactants and polymers on stability and antibacterial activity of silver nanoparticles (NPs). J. Phys. Chem. C 112, 5825–5834.

López-Berges, M.S., Hera, C., Sulyok, M., Schäfer, K., Capilla, J., Guarro, J., Pietro, A.D., 2013. The velvet complex governs mycotoxin production and virulence of *Fusarium oxysporum* on plant and mammalian hosts. Mol. Microbiol. 87, 49.

Malkapur, D., Devi, M.S., Rupula, K., Sashidhar, R.B., 2017. Biogenic synthesis, characterization and antifungal activity of gum kondagogu-silver nano biocomposite construct: assessment of its mode of action. IET Nanobiotechnol. 11, 866–873.

May, R.C., Stone, N.R.H., Wiesner, D.L., Bicanic, T., Nielsen, K., 2016. *Cryptococcus*: from environmental saprophyte to global pathogen. Nat. Rev. Microbiol. 14, 106–117.

Mishra, A., Kumari, M., Pandey, S., Chaudhry, V., Gupta, K.C., Nautiyal, C.S., 2014. Biocatalytic and antimicrobial activities of gold nanoparticles synthesized by *Trichoderma* sp. Bioresour. Technol. 166, 235–242.

Perkas, N., Lipovsky, A., Amirian, G., Nitzan, Y., Gedanken, A., 2013. Biocidal properties of TiO_2 powder modified with Ag nanoparticles. J. Mater. Chem. B 1, 5309–5317.

Pochon, S., Terrasson, E., Guillemette, T., Iacomi-Vasilescu, B., Georgeault, S., Juchaux, M., Berruyer, R., Debeaujon, I., Simoneau, P., Camoion, C., 2012. A model interaction for investigating seed transmission of necrotrophic fungi. Plant Methods 8, 6.

Rispail, N., Matteis, L.D., Santos, R., Miguel, A.S., Custardoy, L., Testillano, P., Risueño, M.C., Pérez-de-Luque, A., Maycock, C., Fevereiro, P., Oliva, A., Fernández-Pacheco, R., Ibarra, M.R., de la Fuente, J.M., Marquina, C., Rubiales, D., Prats, E., 2014. Quantum dot and superparamagnetic nanoparticle interaction with pathogenic fungi: internalization and toxicity profile. ACS-Appl. Mater. Interf. 6, 9100–9110.

Segorbe, A., Di Pietro, E., Pérez-Nadales, D., Turrà, D., 2017. Three *Fusarium oxysporum* mitogen-activated protein kinases (MAPKs) have distinct and complementary roles in stress adaptation and cross-kingdom pathogenicity. Mol. Plant Pathol. 18, 912–924.

Xu, J.R., 2000. Map kinases in fungal pathogens. Fungal Genet. Biol. (3), 137–152.

Xue, D., He, D., Gao, S., Wang, D., Yokoyama, K., Wang, L., 2016. Biosynthesis of silver nanoparticles by the fungus *Arthroderma fulvum* and its antifungal activity against genera of *Candida*, *Aspergillus* and *Fusarium*. Int. J. Nanomedicine 11, 1899–1906.

Yan, S.X., Qing-Tao, S., Shu-Tao, X., Xiu-Lan, C., Cai-Yun, S., Yu-Zhong, Z., 2006. Broad-spectrum antimicrobial activity and high stability of Trichokonins from *Trichoderma koningii* SMF2 against plant pathogens. FEMS Microbiol. Lett. 260, 119–125.

Yu, Y.C., Kuo, C.L., Cheng, W.L., Liu, C.S., Hsieh, M., 2009. Decreased antioxidant enzyme activity and increased mitochondrial DNA damage in cellular models of Machado–Joseph disease. J. Neurosci. Res. 87, 1884–1891.